Tri-Helical Anode Design for Zinc-Iodine Tubular Flow Batteries

Ifeanyi Emmanuel Udom
Department of Electrical and Computer Engineering and Texas Center for Super Conductivity
University of Houston
Houston, Texas, USA
ieudom@uh.edu

Lihong Zhao
Department of Electrical and Computer Engineering and Texas Center for Super Conductivity
University of Houston
Houston, Texas, USA
lzhao26@central.uh.edu

Alae Eddine Lakraychi
Department of Electrical and Computer Engineering Engineering and Texas Center for Super Conductivity
University of Houston
Houston, Texas, USA
alakraychi@central.uh.edu

Yan Yao*
Department of Electrical and Computer Engineering and Texas Center for Super Conductivity
University of Houston
Houston, Texas, USA
*yyao4@central.uh.edu

2025 IEEE Electrical Energy Storage Applications and Technologies Conference (EESAT) | 979-8-3315-2485-2/25/$31.00 ©2025 IEEE | DOI: 10.1109/EESAT62935.2025.10891221

***Abstract*— The global shift towards renewable energy sources necessitates advanced energy storage technologies to ensure a reliable and sustainable electric grid**. **Zinc-iodine flow battery technology shows great promise for scalable energy storage, offering extended cycle life and the ability to independently scale power and energy densities. The tubular cell design enhances electrochemical performance by addressing the limitations associated with traditional planar configurations. However, the zinc wire anode in the tubular design is prone to form Zn dendrites, leading to potential short-circuiting. In this work, we introduce a tri-helical design for zinc anodes that extends cycle life to 250 cycles. Through three-electrode analysis, we found that the tri-helical design enhances the uniformity of zinc plating by improving the anode-electrolyte interface, promoting faster charge transfer, and mitigating dendrite formation. This technology is compatible with existing power infrastructures and supports grid stabilization and integration with renewable energy sources, which offers an exciting pathway for integrating renewable energy systems.**

Keywords: Zinc-Iodine Flow Battery (ZIFB), Energy storage technologies, Dendrite mitigation, Enhanced cycle life, Redox flow batteries, Zinc plating uniformity, Renewable energy grid integration, Battery lifetime enhancement.

I. INTRODUCTION

The global transition to renewable energy sources like solar and wind is essential for achieving a zero-emission future. However, the inherent variability and intermittency of these energy sources pose significant challenges to grid stability. To address these challenges and meet the U.S (United States). goal of integrating 1 terawatt of renewable energy by 2030, covering 80% of annual electricity demand, long-duration energy storage systems are imperative [1-3]. Among various energy storage technologies, redox flow batteries (RFBs) stand out due to their design flexibility, scalability, and high efficiency, making them particularly suitable for large-scale applications [4–13].

Despite progress made with different RFB chemistries, such as all-vanadium and iron-chromium flow batteries [14–18], these systems are often limited by low energy densities compared to lithium-ion batteries (>200 Wh/L).[19]. The widely researched vanadium redox flow battery (VRFB) achieves an energy density of only about 25 Wh/L, largely due to the low solubility of active species in aqueous solutions [20-21]. Furthermore, the high cost of vanadium limits the commercial viability of VRFBs [22-23].

Zinc-iodine flow batteries (ZIFBs) offer a promising alternative, delivering significantly higher theoretical energy densities—up to 322 Wh/L with a high-concentration electrolyte (7 M) [24]. Flow batteries are typically categorized by their design as either planar or tubular. Planar flow batteries feature a flat, stacked configuration with a membrane that separates positive and negative electrolytes. However, this design is often hampered by low power density, high manufacturing costs, and critical issues such as zinc dendrite formation, which severely limit cycle life and overall system reliability [25-26]. In contrast, tubular flow batteries have a cylindrical design, with electrode wires aligned vertically in the cell chamber. The tubular design offers a higher membrane surface area relative to volume, allowing for high flow rates and enhancing the power output of the battery. While this design could achieve higher volumetric power density, it still suffers from issues such as zinc dendrite and short cycle life.

In this work, we introduce a tri-helical zinc anode design to address the anode instability challenge in tubular ZIFBs, which facilitates uniform current distribution, reduces zinc dendrite formation, and allows stable operation over 250 cycles (450 hours). Additionally, this design eliminates the need for traditional planar flow channels and plates, paving the way for cost-effective manufacturing and compatibility with various redox chemistries.

II. METHODOLOGY

We aim to address the critical question: How can the performance and stability of ZIFBs be enhanced through the tri-helical anode design? This question is pivotal in overcoming the current limitations associated with conventional ZIFB systems, particularly the challenges of zinc dendrite formation, limited cycle life, and suboptimal volumetric power density [27].

A. Cell Design and Construction

The electrochemical reactions of the flow battery are shown in following equations: [14]

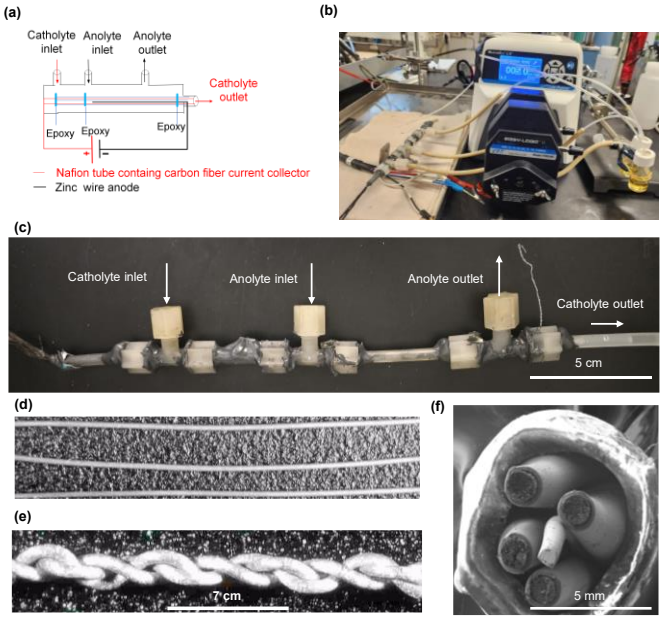

Fig. 1. **Tubular flow battery design architecture**. (a) Schematic showing flow paths of catholyte and anolyte in a tubular ZIFB. (b) The tubular ZIFB set up. (c) Tubular flow cell assembled with tubular 3 frame and tubes(d) Cylindrical zinc anode. (e) Tri-helical zinc anode. (f) Tubular cell geometry with four Nafion tubes, each containing a carbon fiber core as the cathode current collector.

Cathode:

$$I_3^- + 2e^- \rightarrow 3I^- \; E° = 0.53\,V \text{ vs SHE} \quad (1)$$

Anode:

$$Zn \rightarrow Zn^{2+} + 2e^- \; E° = -0.76\,V \text{ vs SHE} \quad (2)$$

Overall:

$$I_3^- + Zn \rightarrow 3I^- + Zn^{2+} \quad E = 1.29\,V \quad (3)$$

The tri-helical tubular ZIFB was constructed using three tube-shaped frames connected by small plastic tubes following the schematic shown in **fig. 1a**. The assembled cell and entire pumping system are shown in **fig. 1b–c**. Zinc wires (0.25mm diameter from Goodfellow) served as the anode and carbon fibers wrapped in four Nafion microtubular membranes were used as the cathode current collector. All components were fixed within the frames using waterproof and chemically resistant epoxy glue (J-B Weld).

The assembly of the tri-helical tubular ZIFB module followed a multi-step process. Initially, four equal-weight carbon fibers were placed into the Nafion microtubular membranes, with a portion of the fibers left exposed for electrical connections. These prepared membranes were then inserted into a polytetrafluoroethylene (PTFE) tubing and positioned within the first of three compression frames, with the carbon fiber end centered to facilitate liquid flow. Both ends of this frame were sealed with epoxy to prevent leaks.

Next, two types of zinc anodes were prepared. The tri-helical anode was created by twisting three zinc wires together along the axial direction. For comparison, the cylindrical anode was prepared by aligning three zinc wires side by side in parallel. The microtubular membranes and a zinc anode were inserted into another PTFE tubing and a second tubular frame. Then, all components were inserted into a long PTFE tubing connected to the electrolyte reservoir. The optical Here, n represents the number of electrolyte volumes participating in the reaction. For this system, n =1, because the anolyte does not participate in the redox reaction, and only the catholyte contributes to the reaction. image and cross-sectional scanning electron micrograph (SEM) of the cells with tri-helical and cylindrical anodes are shown in **fig. 1d–f**. The length of active components in the chamber was fixed to 5 cm to ensure consistency. The terminals of carbon fiber and zinc electrodes were wrapped with copper foil and sealed with silver paste to reduce contact resistance. After curing the glue for 12 hours and checking for leaks, the ZIFB cell was ready for operation. 6 mL of 2 M ZnI_2 solution is used as catholyte and anolyte, respectively. Volume of the cell chamber is 0.158 ml.

B. Electrochemical Measurements

In an operating battery, the catholyte and anolyte composed of the zinc iodine flow from the left inlets into the cell chamber as indicated in **fig. 1a and c**. The electrolyte after reaction returns to the external reservoir through the right outlet. The flow rate is controlled by a peristaltic pump (Cole-Parmer) and its actual value is calibrated with a flow transducer from Omega that senses 20 to 100 mL/m flow rate of liquid (model number is FLR1001). The potentiostat used was Biologic VMP3. Electrochemical impedance spectroscopy (EIS) was carried out from 100 kHz to 100 MHz at 10 mV amplitude. Galvanostatic cycling was performed at a current of 40 mA for constant capacity of 214 mAh, which is 50% of theoretical capacity of catholyte. For the longevity test, galvanostatic cycling with constant capacity is set to 10 mAh per cycle with a charge and discharge cutoff voltages of 1.6 V and 0.25V, respectively.

III. RESULTS AND DISCUSSION

A. Energy Density of Tubular Cells

The energy and power density of the tubular cell are calculated and compared with ZIFB counterparts with planar design. The energy density (E) of a RFB is the amount of energy stored per unit volume of electrolyte. It can be described by the concentration of active redox species (C_a) and voltage (V) in the form of Equation 4:

$$E = \frac{NC_aFV}{n} \quad (4)$$

where N is the number of electrons involved in the redox reaction. F is the Faraday constant and n is the effective number of electrolyte volumes actively participating in redox reactions.This parameter accounts for the fraction of the total electrolyte volume directly involved in the electrochemical processes. In our zinc-iodine flow battery system, we have two distinct electrolyte volumes, the anolyte and the catholyte. However, only the catholyte actively contributes to the redox reactions occurring at the electrodes, as the anolyte primarily serves to facilitate ionic transport without undergoing direct redox activity. As such, the equivalent number of electrolyte volumes, n, is defined as 1 in our system because only the catholyte participates in the reaction. Theoretical energy density is 92 Wh L^{-1} based on Ca= 2M, N= 4/3, V=1.29V. [29].

B. Flow Rate Optimization

To quantify the impact of varying electrolyte flow rates on battery performance, a flow transducer was employed. This device was critical in measuring the actual flow rates exiting

the Nafion membrane, revealing that the true flow rate exiting the system was 19 ml/min, which was less that what was displayed in the prismatic pump. Experiments demonstrated that increasing the flow rate helps achieve high discharge capacity within a certain threshold. as shown in **fig. 2**, underscoring the importance of maintaining precise control flow rate to optimize battery performance.

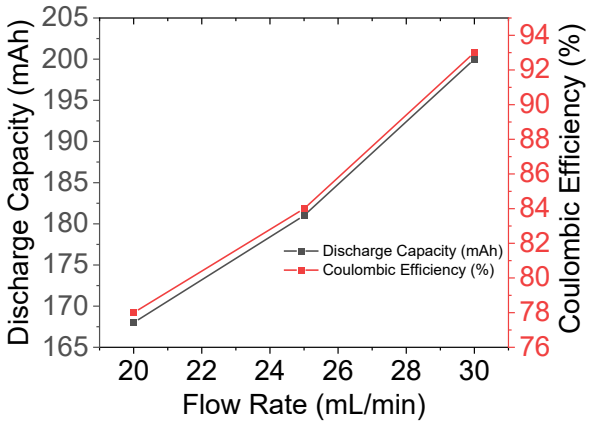

Fig. 2. **Flow rate vs Coulombic efficiency and capacity**.

C. *Electrochemical Performance of Tubular ZIFB*

The tri-helical zinc anode demonstrate a significant improvement in electrochemical performance compared to cylindrical anode designs in terms of electrode overpotential and cycle life. **fig. 3a-c** shows the voltage, capacity retention and efficency metrics of tubular cells with tri-helical and cylindrical anodes.

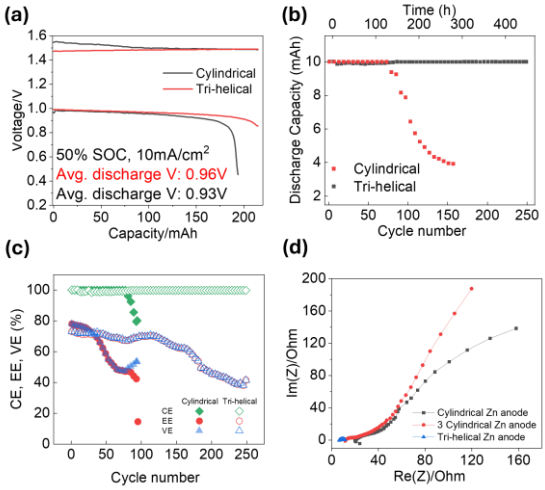

Fig. 3. **Electrochemical performance**. (a) Voltage vs capacity of Tri-helical and three cylindrical zinc anodes in ZIFB at 0-50% SOC. (b) Discharge capacity vs cycle for Tri-helical and three cylindrical Zinc anode in ZIFB with 10 mAh capacity (0-2.3% SOC). (c) Coulombic efficiency (CE), energy efficiency (EE) and voltage efficiency (VE) vs cycle number of Tri-helical and three cylindrical Zinc anode in ZIFB. (d) EIS of Tri-helical one cylindrical and three cylindrical zinc anodes in ZIFB.

The charge overpotential of trihelical anode is 10mV lower than cylindrical anode counterparts (**supplementary fig. S2**), suggesting a smaller internal resistance during zinc plating reaction.

In addition to lower overpotential, tri-helical zinc anode also enables better cycling stability. The capacity retention profile of the tri-helical anode **(fig. 3a**) remained stable with minimal fluctuation, indicating a consistent electrochemical environment throughout the cycling process. In contrast, the cylindrical anode configurations showed instability, particularly after prolonged cycling, suggesting increased internal resistance due to non-uniform zinc stripping and plating. In longtevity tests at 10mAh per cycle, the tri-helical configuration achieved 250 stable cycles, which translates to over 450 hours of continuous operation **(fig. 3b).** In contrast, the cylindrical anode cell experienced a rapid capacity decay at the 76th cycle. This extended cycle life is attributed to the improved current distribution and uniform zinc plating facilitated by the tri-helical design. Additionally, the efficiency metrics (**fig. 3c**) highlight the higher Coulombic, energy, and voltage efficiencies of tri-helical anode, underscoring the effectiveness of this electrode design. Finally, the EIS data in **fig. 3d** reveal the reduced internal resistance of the tri-helical anode.

D. *Dendrite Mitigation and Zinc Plating Morphology*

The lower overpotential and improved cycle life with tirhelical anode can be attributed to the uniform zinc deposition. The optical image of zinc anodes after cycling is shown in **fig. 4a and b**. Massive dendrites were observed on zinc wires in cylindrical anodes as shown in **fig. 4a.**

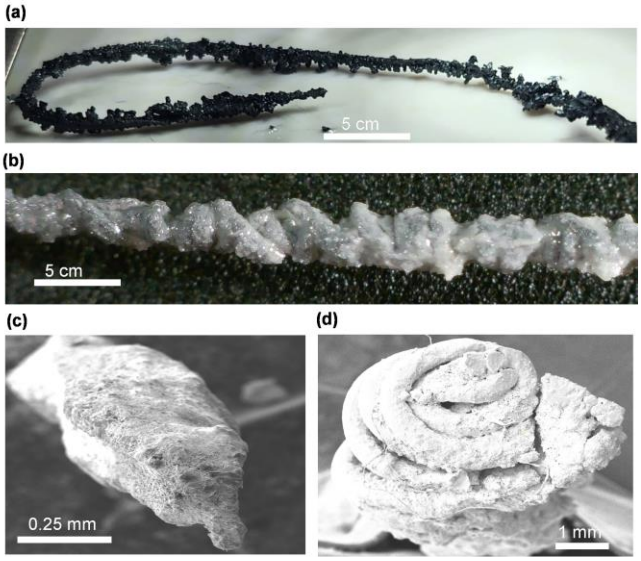

Fig. 4. **Zinc anode and plating morphology.** (a) Microscopic view of cylindrical zinc anode. (b) Microscopic view of tri-helical zinc anode. (c) Scanning Electron Microscopy (SEM) view of cylindrical zinc anode after cycling (d) SEM view of Tri-helical Zinc Anode after cycling.

The maximum height of the dendrite reached 0.186 inch (**supplementary fig. S3)**, The tri-helical zinc anode exhibited a marked reduction in dendrite formation compared to the cylindrical and three parallel zinc anodes. Post-cycling analysis using SEM revealed a significantly smoother surface on the tri-helical anode, with fewer and smaller dendritic structures **(fig. 4d**). This contrasts sharply with the cylindrical anode, where extensive dendrite growth was observed. Dendrite formation occurs due to uneven current distribution, creating localized hotspots of high current density that promote rapid and uncontrolled zinc deposition. Over

successive charge-discharge cycles, these needle-like dendrites grow progressively longer and sharper. In the context of the tubular flow battery system, this growth poses a significant risk as the dendrites can penetrate the Nafion-based tubing, which acts as the separator between the anolyte and catholyte. Such penetration compromises the integrity of the separator, leading to internal short circuits and the mixing of electrolytes. This not only results in catastrophic battery failure but also significantly reduces its operational lifespan and safety. The tri-helical design mitigates this issue by promoting uniform current distribution, effectively suppressing dendrite growth and maintaining the structural integrity of the Nafion-based tubing.and reduced battery life **(fig. 3b, and 4a).** The uniform current distribution provided by the tri-helical design was instrumental in achieving even zinc plating, as evidenced by the SEM images**(fig. 4d).** The improved morphology of the zinc plating on the tri-helical anode is a crucial factor contributing to the enhanced cycle life and overall stability of the battery. As shown in **fig. 3b**, the plating morphology on the tri-helical zinc anode demonstrates a significantly surface with fewer and smaller dendritic structures compared to the cylindrical anode **(fig. 4a).**

E. Impact of Flow Rate on Battery Performance

The effect of electrolyte flow rate on the performance of the zinc-iodine flow battery was systematically investigated. The results show that the tri-helical anode configuration allowed a higher tolerance to variations in flow rate, with the optimal flow rate identified at approximately 30 mL/min (Figure 2). At this flow rate, the battery exhibited the highest coulombic efficiency, with a significant reduction in overpotential. This optimization is crucial for scaling up the system for larger applications, as it ensures that the battery can operate efficiently under different operating conditions.

Increasing the flow rate beyond the optimal point, however, led to a decrease in capacity retention. This decline is likely due to the excessive shear force acting on the electrolyte, which can disrupt the uniformity of the electrochemical reactions and lead to inefficiencies. Therefore, maintaining the flow rate within the optimal range is critical for preserving battery performance.

F. Voltage Efficiency and Power Density

The voltage efficiency of the tri-helical zinc-iodine flow battery was significantly higher than that of the cylindrical design. The tri-helical configuration achieved a power density of 4.4 W/L, a substantial improvement over the conventional designs.

The increased surface area-to-volume ratio provided by the tri-helical design allows for more efficient ion transfer and reduces the overall impedance of the cell. This reduction in impedance was confirmed by the EIS data, which showed lower resistance values for the tri-helical anode compared to the cylindrical and parallel anode designs **(fig. 5d**). The higher voltage efficiency and power density(**fig. 5c)** make the tri-helical design particularly well-suited for applications requiring high power output and long-term energy storage.

G. Challenges at cell level

The long-term stability of the tri-helical anode under varying environmental conditions requires further investigation. Additionally, the scalability of this design for industrial applications, particularly in terms of manufacturing and cost-effectiveness, remains a challenge that needs to be addressed in future research. This work also highlights the need for further study the impact of different flow rates on dendrite formation and zinc plating uniformity also warrants more detailed investigation to fully understand the underlying mechanisms. the tri-helical zinc-iodine flow battery a promising candidate for large-scale energy storage, particularly for integrating renewable energy sources into the grid. Future research should focus on optimizing the electrolyte flow and composition, refining flow rates, pressure drops and exploring alternative anode materials to enhance performance and scalability. I.

IV. CONCLUSION

In this work, we introduced and evaluated the tri-helical zinc anode design for zinc-iodine tubular flow batteries, addressing critical challenges in energy storage. The tri-helical configuration demonstrated a 72% increase in cycling time, translating to 250 cycles, improved zinc plating uniformity, and significant reduction in dendrite formation. These improvements enhance the stability and efficiency of the battery system, with the tri-helical anode outperforming conventional cylindrical and parallel designs. The optimized current distribution achieved by the tri-helical structure reduced internal resistance and increased electrochemical efficiency, resulting in higher capacity retention, voltage efficency, energy efficiency and power density. Future research should focus on optimizing the electrolyte flow and composition, refining flow rates, pressure drop and exploring alternative anode form factors to enhance performance and scalability. Furthermore, the tri-helical zinc-iodine flow battery (ZIFB) presents environmental advantages. Zinc, an abundant and widely available material, reduces dependence on rare resources like cobalt and lithium. The aqueous electrolyte used in ZIFBs further reduces environmental impact by eliminating organic solvents, minimizing fire hazards, and reducing toxicity risks. These factors position ZIFBs as a promising, environmentally friendly alternative for large-scale, long-duration energy storage systems

ACKNOWLEDGMENT

I.E.U. acknowledges Mush Khan and Maleek Andrew from Alchemy Industrial LLC, Kelvin Meagher From Sun Company and Dr. Guang Yang from Oak Ridge National Laboratory (ORNL) for helpful discussions.

REFERENCES

[1] S. Chu, Y. Cui, and N. Liu, "The path towards sustainable energy," Nature Materials, vol. 16, no. 1, pp. 16-22, Dec. 2016, doi: 10.1038/nmat4834

[2] Center for Sustainable Systems, University of Michigan. 2023. "U.S. Renewable Energy Factsheet." Pub. No. CSS03-12.

[3] The White House, "The Long-Term Strategy of the United States: Pathways to Net-Zero Greenhouse Gas Emissions by 2050," Washington, DC, USA, Oct. 2021. [Online]. Available: https://www.whitehouse.gov/wp-content/uploads/2021/10/us-long-term-strategy.pdf

[4] M. Skyllas-Kazacos, M. H. Chakrabarti, S. A. Hajimolana, F. S. Mjalli, and M. Saleem, "Progress in flow battery research and development," J. Electrochem. Soc., vol. 158, pp. 7–10, 2011 .

[5] W. Wang, Q. Luo, B. Li, X. Wei, L. Li, and Z. Yang, "Recent progress in redox flow battery research and development," Adv. Funct. Mater., vol. 23, pp. 970–986, 2013.

[6] P. Alotto, M. Guarnieri, and F. Moro, "Redox flow batteries for the storage of renewable energy: a review," Renew. Sustain. Energy Rev., vol. 29, pp. 325–335, 2014.

[7] G. L. Soloveichik, "Flow batteries: current status and trends," Chem. Rev., vol. 115, pp. 11533–11558, 2015.

[8] M. Park, J. Ryu, W. Wang, and J. Cho, "Material design and engineering of next-generation flow-battery technologies," Nat. Rev. Mater., vol. 2, pp. 1–18, 2016.

[9] M. L. Perry and A. Z. Weber, "Advanced redox-flow batteries: a perspective," J. Electrochem. Soc., vol. 163, pp. A5064–A5067, 2016.

[10] Q. Huang and Q. Wang, "Next-generation, high-energy-density redox flow batteries," Chempluschem, vol. 80, pp. 312–322, 2015.

[11] W. Lu, X. Li, and H. Zhang, "The next generation vanadium flow batteries with high power density - A perspective," Phys. Chem. Chem. Phys., vol. 20, pp. 23–35, 2017.

[12] B. Li and J. Liu, "Progress and directions in low-cost redox-flow batteries for large-scale energy storage," Natl. Sci. Rev., vol. 4, pp. 91–105, 2017.

[13] C. Ponce de León, A. Frías-Ferrer, J. González-García, D. A. Szántó, and F. C. Walsh, "Redox flow cells for energy conversion," J. Power Sources, vol. 160, pp. 716–732, 2006.

[14] L. Wei, C. Xiong, H. R. Jiang, X. Z. Fan, and T. S. Zhao, "Highly catalytic hollow Ti3C2Tx MXene spheres decorated graphite felt electrode for vanadium redox flow batteries," Energy Storage Mater., vol. 25, pp. 885–892, 2020.

[15] H. R. Jiang, J. Sun, L. Wei, M. C. Wu, W. Shyy, and T. S. Zhao, "A high power density and long cycle life vanadium redox flow battery," Energy Storage Mater., vol. 24, pp. 529–540, 2019.

[16] H. R. Jiang, B. W. Zhang, J. Sun, X. Z. Fan, W. Shyy, and T. S. Zhao, "A gradient porous electrode with balanced transport properties and active surface areas for vanadium redox flow batteries," J. Power Sources, vol. 440, p. 227159, 2019.

[17] Y. K. Zeng, T. S. Zhao, X. L. Zhou, L. Wei, and H. R. Jiang, "A low-cost iron-cadmium redox flow battery for large-scale energy storage," J. Power Sources, vol. 330, pp. 55–60, 2016.

[18] Y. K. Zeng, T. S. Zhao, X. L. Zhou, L. Zeng, and L. Wei, "The effects of design parameters on the charge-discharge performance of iron-chromium redox flow batteries," Appl. Energy, vol. 182, pp. 204–209, 2016.

[19] M. S. Whittingham, "History, evolution, and future status of energy storage," Proc. IEEE, vol. 100, pp. 1518–1534, 2012

[20] K. Lourenssen, J. Williams, F. Ahmadpour, R. Clemmer, and S. Tasnim, "Vanadium redox flow batteries: a comprehensive review," J. Energy Storage, vol. 25, p. 100844, 2019.

[21] Y. K. Zeng, T. S. Zhao, L. An, X. L. Zhou, and L. Wei, "A comparative study of all-vanadium and iron-chromium redox flow batteries for large-scale energy storage," J. Power Sources, vol. 300, pp. 438–443, 2015.

[22] D. S. Aaron, Q. Liu, Z. Tang, G. M. Grim, A. B. Papandrew, A. Turhan, T. A. Zawodzinski, and M. M. Mench, "Dramatic performance gains in vanadium redox flow batteries through modified cell architecture," J. Power Sources, vol. 206, pp. 450–453, 2012.

[23] L. Li, S. Kim, W. Wang, M. Vijayakumar, Z. Nie, B. Chen, J. Zhang, G. Xia, J. Hu, G. Graff, J. Liu, and Z. Yang, "A stable vanadium redox-flow battery with high energy density for large-scale energy storage," Adv. Energy Mater., vol. 1, pp. 394–400, 2011.

[24] B. Li, Z. Nie, M. Vijayakumar, G. Li, J. Liu, V. Sprenkle, and W. Wang, "Ambipolar zinc-polyiodide electrolyte for a high-energy density aqueous redox flow battery," Nat. Commun., vol. 6, no. 6303, Feb. 2015.

[25] Y. Wu, F. Zhang, T. Wang, P.-W. Huang, A. Filippas, H. Yang, Y. Huang, C. Wang, H. Liu, X. Xie, R. P. Lively, and N. Liu, "A submillimeter bundled microtubular flow battery cell with ultrahigh volumetric power density," Proc. Natl. Acad. Sci. U.S.A., vol. 119, no. 49, Nov. 2022.

[26] Q. P. Jian, M. C. Wu, H. R. Jiang, Y. K. Lin, and T. S. Zhao, "A trifunctional electrolyte for high-performance zinc-iodine flow batteries," Journal of Power Sources, vol. 484, p. 229238, 2021, doi: 10.1016/j.jpowsour.2020.229238.[Online].Available:https://www.sciencedirect.com/science/article/pii/S0378775320315275.

[27] S. J. Banik and R. Akolkar, "Suppressing Dendritic Growth during Alkaline Zinc Electrodeposition using Polyethylenimine Additive," Electrochimica Acta, vol. 165, pp. 1-10, Oct. 2015. doi: 10.1016/j.electacta.2014.12.100.

[28] J. Su, J. Ye, Z. Qin, and L. Sun, "Polytetrafluoroethylene Modified Nafion Membranes by Magnetron Sputtering for Vanadium Redox Flow Batteries," Coatings, vol. 12, no. 3, p. 378, Mar. 2022. doi: 10.3390/coatings12030378.

[29] T. Zhang and S. L. Suib, "Chem. Rev.," vol. 115, no. 22, pp. 11533−115,

SUPPLEMENTARY INFORMATION

Tri-Helical Anode Design for Zinc-Iodine Tubular Flow Batteries

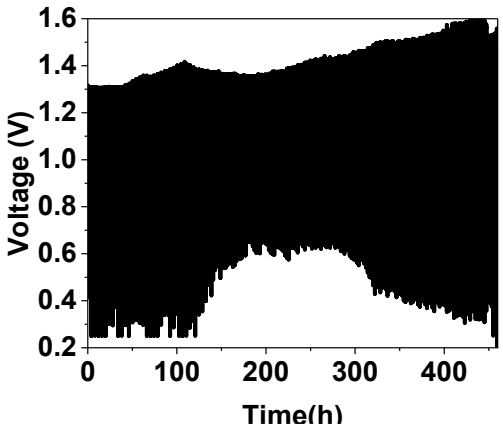

Supplementary Figure 1. Voltage vs time for Tri-helical and three cylindrical Zinc anode in ZIFB with 10 mAh capacity (0-2.3% SOC).

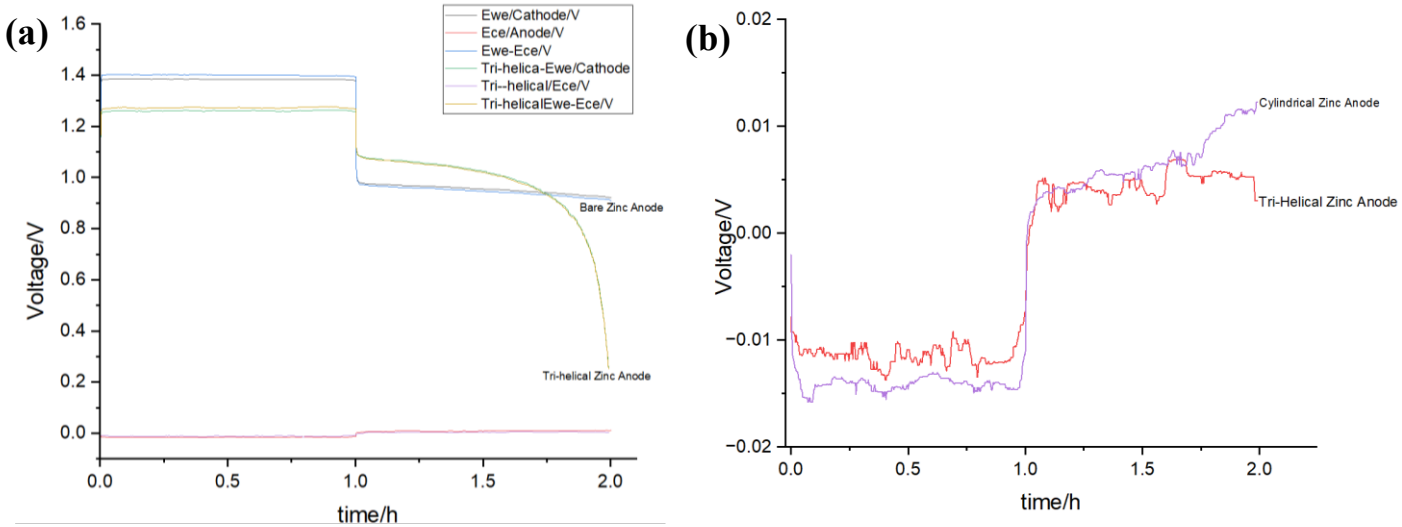

Supplementary Figure 2. (a) Three-electrode measurement of tri-helical Zinc vs conventional anode at 10mA cycling. (b) magnified view of the anode.

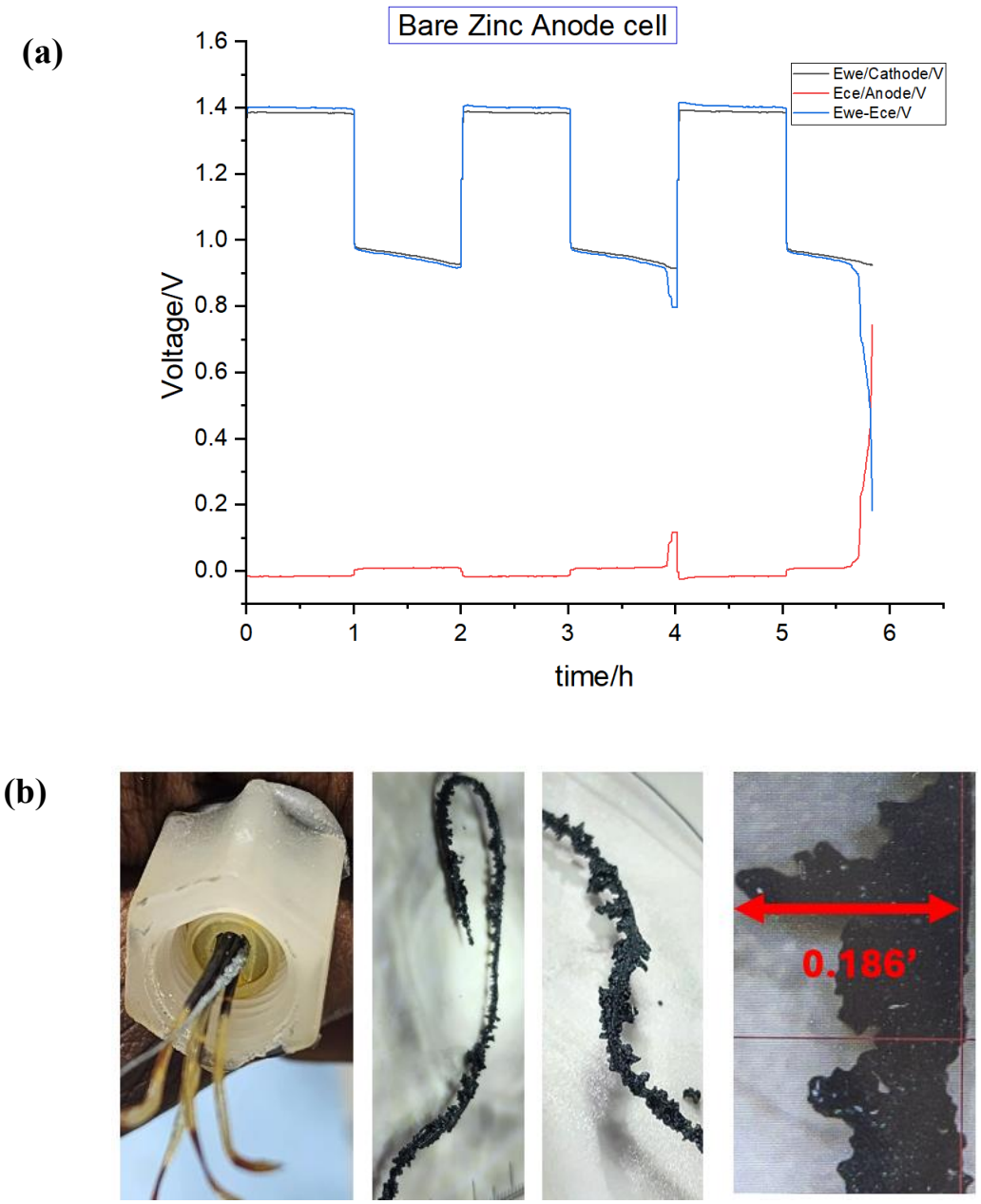

Supplementary Figure 3. (a) Three-electrode test shows cell failure at 5.8 hour due to the failure of the anode. (b) Tear-down optical images of the flow cell after shorting.